frontiers in Earth Science

ORIGINAL RESEARCH
published: 02 March 2022
doi: 10.3389/feart.2022.850633

Quantitative Reconstruction of Precipitation and Lake Areas During Early to Middle Holocene in Mu Us Desert, North China

Dawei Li[1], *Yongqiu Wu*[2]*, *Lihua Tan*[1], *Yanglei Wen*[1] *and Tianyang Fu*[1]

[1]State Key Laboratory of Earth Surface Processes and Resource Ecology, Beijing Normal University, Beijing, China, [2]College of Geography and Environmental Sciences, Zhejiang Normal University, Jinhua, China

Paleoclimatic researches have revealed that the East Asian summer monsoon (EASM) strengthened and precipitation increased in north China during the early to middle Holocene. The lacustrine landform and sediment recorded approximately simultaneous Holocene high lake levels. However, relatively few studies have been reported involving the quantitative reconstruction of precipitation and lake areas in the Mu Us Desert (MUD), northwest edge area of the modern EASM. Based on the lacustrine landform, and by using the lake hydrologic model, this study quantitatively reconstructed precipitation and lake areas during the early to middle Holocene in the MUD. The results revealed the following: 1) A total of 127 paleolakes existed in the closed drainage area during the early to middle Holocene. The area of paleolakes was 896.1 km^2, which is 2.96 times that of modern lakes. The relative height between the highstand and the modern lake surface is ~5–9 m. 2) Precipitation during the early to middle Holocene decreased from 550 mm in the southeast to 350 mm in the northwest. The 400 mm isohyet moved 130–170 km to the northwest, roughly coincident with the modern 250 mm isohyet. 3) The relative increase in precipitation was ~32–60%, and the increase in the west was significantly higher than in the east. The precipitation gradient in much of the MUD was lower than the present. The results show that the monsoon edge area and monsoon rain belt migrated to the northwest during the early to middle Holocene. The MUD was stably dominated by the EASM. Data also showed that the spatio-temporal pattern of the climate during the early to middle Holocene was relatively humid with a decreased precipitation gradient for millennia.

Keywords: Mu Us Desert, closed drainage area, early to middle Holocene, quantitative precipitation reconstruction, lake area

OPEN ACCESS

Edited by:
Zhuolun Li,
Lanzhou University, China

Reviewed by:
Xiaokang Liu,
Shaanxi Normal University, China
Li Wu,
Anhui Normal University, China

***Correspondence:**
Yongqiu Wu
wuyongqiu@zjnu.edu.cn

Specialty section:
This article was submitted to Quaternary Science, Geomorphology and Paleoenvironment, a section of the journal Frontiers in Earth Science

Received: *07 January 2022*
Accepted: *04 February 2022*
Published: *02 March 2022*

Citation:
Li D, Wu Y, Tan L, Wen Y and Fu T (2022) Quantitative Reconstruction of Precipitation and Lake Areas During Early to Middle Holocene in Mu Us Desert, North China. Front. Earth Sci. 10:850633. doi: 10.3389/feart.2022.850633

INTRODUCTION

There were variations in monsoon precipitation in the geological data recorded in China during the Holocene (An et al., 2000). The data showed that the East Asian summer monsoon (EASM) strengthened, the monsoon rain belt moved northwestward, and precipitation increased in the early to middle Holocene (Yang et al., 2015a). Holocene precipitation variations in north China have been quantitatively reconstructed with multiple methods. In the Chinese Loess Plateau, Sun et al. (1995) established a susceptibility-rainfall conversion function by regression analysis of magnetic susceptibility of surface soils and contemporary precipitation data. The reconstructed

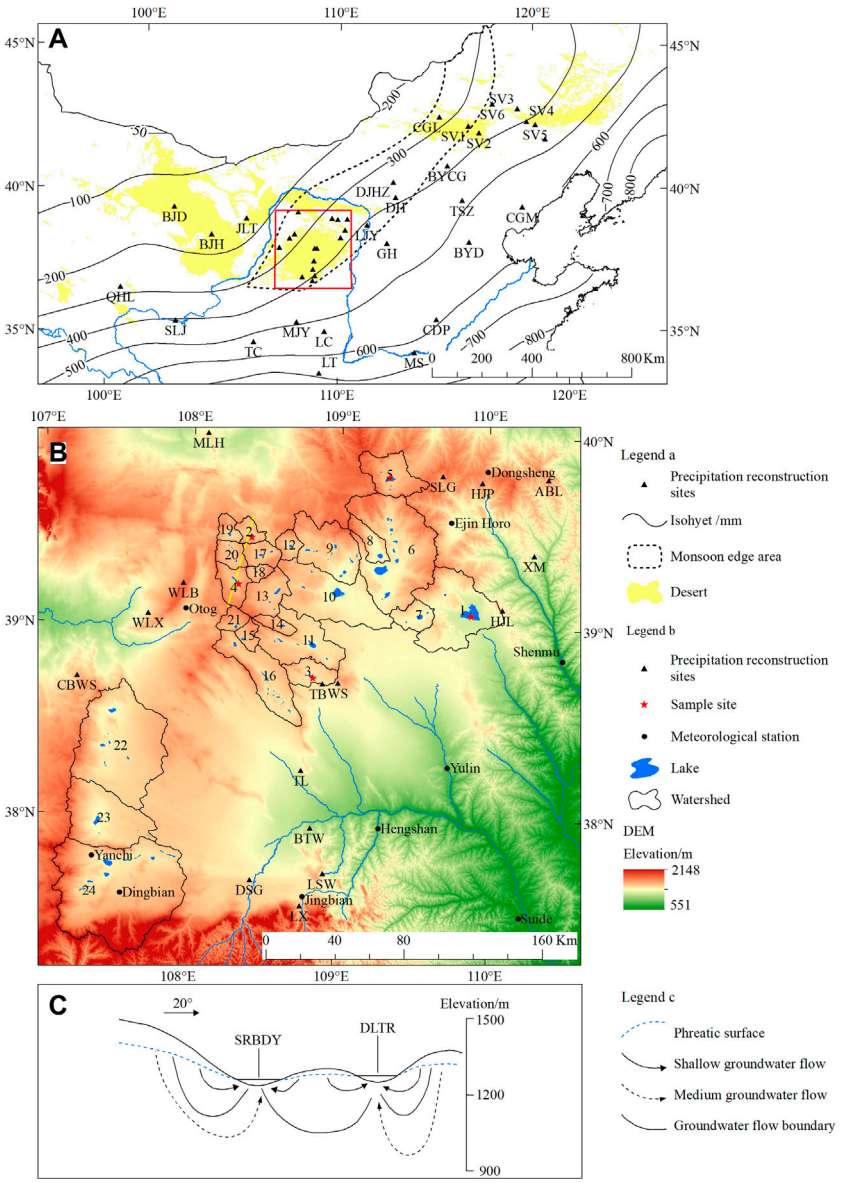

FIGURE 1 | Overview of the study area. **(A)** Map of northern China and location of study area. The modern isohyets are values averaged over 56 years (1961–2016); monsoon edge area is modified after Zhang et al. (1993); the red rectangle is the study area. **(B)** Topography of study area. The DEM data is from ASTER GDEM version2. **(C)** Diagrammatic section of groundwater flow system of SRBDY–DLTR Nuur drainage areas (modified after Hou et al., 2008); location of the section is shown by the yellow line in **Figure 1B**).

precipitation was 100–150 mm higher than the present in the loess-desert transitional zone during the Holocene optimum. Precipitation reconstruction from the Gonghai Lake in the north loess plateau revealed gradually increasing rainfall since the last deglaciation, reaching a maximum of 30% higher than the present during the middle Holocene (Chen et al., 2015). In eastern Inner Mongolia Plateau, pollen records of Chagan Nuur showed that the East Asian monsoon precipitation began to increase in the early Holocene and reached a maximum in the middle Holocene, which was 30–50% higher than modern rainfall (Li et al., 2020). The lake hydrologic model and Holocene shoreline records were used to reconstruct the precipitation in Dali Lake, located near the northwestern limit of the EASM domain. The results showed that rainfall in the Dali Lake area increased by 11–5.5 ka, and the EASM expanded northwest (Goldsmith et al., 2017). The Bayanchagan Lake in southern Inner Mongolia also recorded a wet period in the early to middle Holocene, with annual precipitation approximately 32% higher than the present (Jiang et al., 2006). In the Alxa Plateau, the reconstructed average precipitation of the Jilantai playa during 8.5–3.5 ka was 246 mm, about 75% higher than the present (Wu et al., 2018). In the Badain Jaran Desert, Yang and

Williams (2003) estimated precipitation of ~200 mm during the early to middle Holocene, at least twice that of the modern period. The reconstructed precipitation in the Shiyang River drainage area during the middle Holocene was approximately 70% higher than the present (Liu and Li, 2017). The reconstruction results showed that the increase percentage in precipitation during the early to middle Holocene ranged from ~30% to 100% compare with the present in north China, with significant differences near the northwestern limit of the EASM domain.

Lakes are treated as archives of earth history (Cohen, 2003). In structurally stable regions, lake level fluctuation is a sensitive response to catchment climatic change (Fritz, 2008). According to the quantitative reconstruction results, the climate in the early to middle Holocene was wetter than the present. Furthermore, the lacustrine landform and strata show the lakes' highstand during this period. For instance, the lacustrine strata revealed by cores in the Ulan Buh Desert show that a unified paleolake developed in the northern part of the desert during the early to middle Holocene (Chen et al., 2014). The lake highstand in Badain Jaran Desert occurred at ~10–6.6 cal ka BP (Wang et al., 2016). Evidence from ancient shorelines and lacustrine stratigraphy in Badain Jaran Desert indicate that the area of the lakes during this period was about five times that of modern lakes (Yang and Williams, 2003). The terrace of Baijian lake in Tengger Desert shows the lake level was ~15 m higher than present at 8.5–5.1 ka (Zhang et al., 2004). Furthermore, lacustrine landform and strata recorded the existence of lake highstands during the early and middle Holocene in the south and east Inner Mongolia Plateau (Yang et al., 2011; Yang et al., 2015b; Zhang et al., 2016).

The Mu Us Desert (MUD) is one of the twelve sandy areas in China. It is located northwest edge area of the modern EASM (**Figure 1A**). Precipitation reconstruction is of great significance to the study of climate change in the EASM edge area and the evolution of the MUD. In addition, it is beneficial to understand the desert's evolution and landform pattern by reconstructing paleolake area during the early to middle Holocene. Previous research has mainly focused on sediments in the southeast of the desert. Moreover, paleoclimatic records have been revealed from the aeolian sand-paleosol sequence, loess-paleosol sequence, and alluvial-lacustrine-peat deposition (Gao et al., 1993; Zhou et al., 1999; Jia et al., 2015; Liu et al., 2018a; Jia et al., 2018). Proxies such as magnetic susceptibility and pollen assemblage have been used to quantitatively reconstruct precipitation levels (Shi et al., 1988; Chen et al., 1993; Sun and Feng, 2013; Liu et al., 2017). The paleoclimatic research in the northwest of the desert has received relatively less attention. Moreover, current studies rarely involve the reconstruction of the paleolake area in the desert. Here, this study presents and discusses reconstructed precipitation and lake areas during the Holocene highstand based on the lakes in the closed drainage area of the west and north MUD.

REGIONAL SETTING

The MUD, with an area of about 4×10^4 km^2, is situated in the southeastern Ordos Plateau. Elevation ranges from 1600 m a.s.l. in the northwest to 1,200 m in the southeast. Bedrock hills from the arid denudation plateau in the northwest MUD extend to the southeast. Lakes and alluvial-lacustrine plains are distributed in valleys between bedrock hills. The aeolian landform presents a characteristically staggered distribution pattern of different forms of mobile, semi-fixed, and fixed dunes/land (Department of Geography of Peking University, 1983). The underlying bedrock in the MUD is Jurassic and Cretaceous sandstone, of which the weathered detritus provide one of the major provenances of the desert(Zhu et al., 1980). The mean annual precipitation decreased by about 450 mm to the northwest. Dominated by the East Asian monsoon, 60–70% of the annual rainfall occurs between July and September. The mean annual temperature ranges from 6.5 to 9°C.

There are 154 natural lakes in the MUD covering an area ≥0.1 km^2(Wu et al., 2017). Most of the lakes are distributed in bedrock valleys or aeolian depressions. Jurassic and Cretaceous sandstone constitute the lake floor. These lakes are salt lakes with a mineral concentration ranging from 75 to 400 g/L, except for some freshwater or brackish water lakes such as Hongjian Nuur and Daotuhaizi in the southeast MUD(Zheng et al., 1992). The average depth of most lakes is within 2 m. Hongjian Nuur is the deepest lake with an average depth of 8.2 m at 1230 m a.s.l (Wang and Dou, 1998). Groundwater resources in MUD are abundant with a salinity less than 1 g/L. The groundwater table in the inter-dune depressions is within 1 m (Department of Geography of Peking University, 1983). The lakes are convergent centers of surface and groundwater runoff in local watershed (Hou et al., 2005).

The west and north MUD belong to the Ordos Plateau closed drainage area, showing neither surface nor groundwater hydraulic connection with the Yellow River and its tributaries (Hou et al., 2008). There are 108 natural lakes distributed in closed drainage area. The total area of these lakes is 301.1 km^2. These lakes can be divided into twenty-four drainage basins according to surface watershed (**Figure 1B**). The surface watershed is approximately consistent with the groundwater watershed (Hou et al., 2005). Each basin contains a single lake or catenulated lakes connected by seasonal river channels. Groundwater renewal ability decreases with depth in the closed drainage area. The annual renewal rate of medium and deep groundwater flow is less than 0.5% and 0.02%, respectively. The vertical hydraulic connection between shallow groundwater and medium to deep groundwater is weak (Wan et al., 2010). Therefore, the lakes in each drainage basin are independent discharge centers of surface runoff and shallow groundwater flow (**Figure 1C**).

MATERIALS AND METHODS

Lacustrine Landform and Sample

Lacustrine plains, lake terraces, and lake shorelines are the landform relics of lake evolution. The lake terrace relics and corresponding lacustrine deposits, which represent the stable stage of lakes during their expansion period, are direct evidence of the evolutionary history of lakes and for

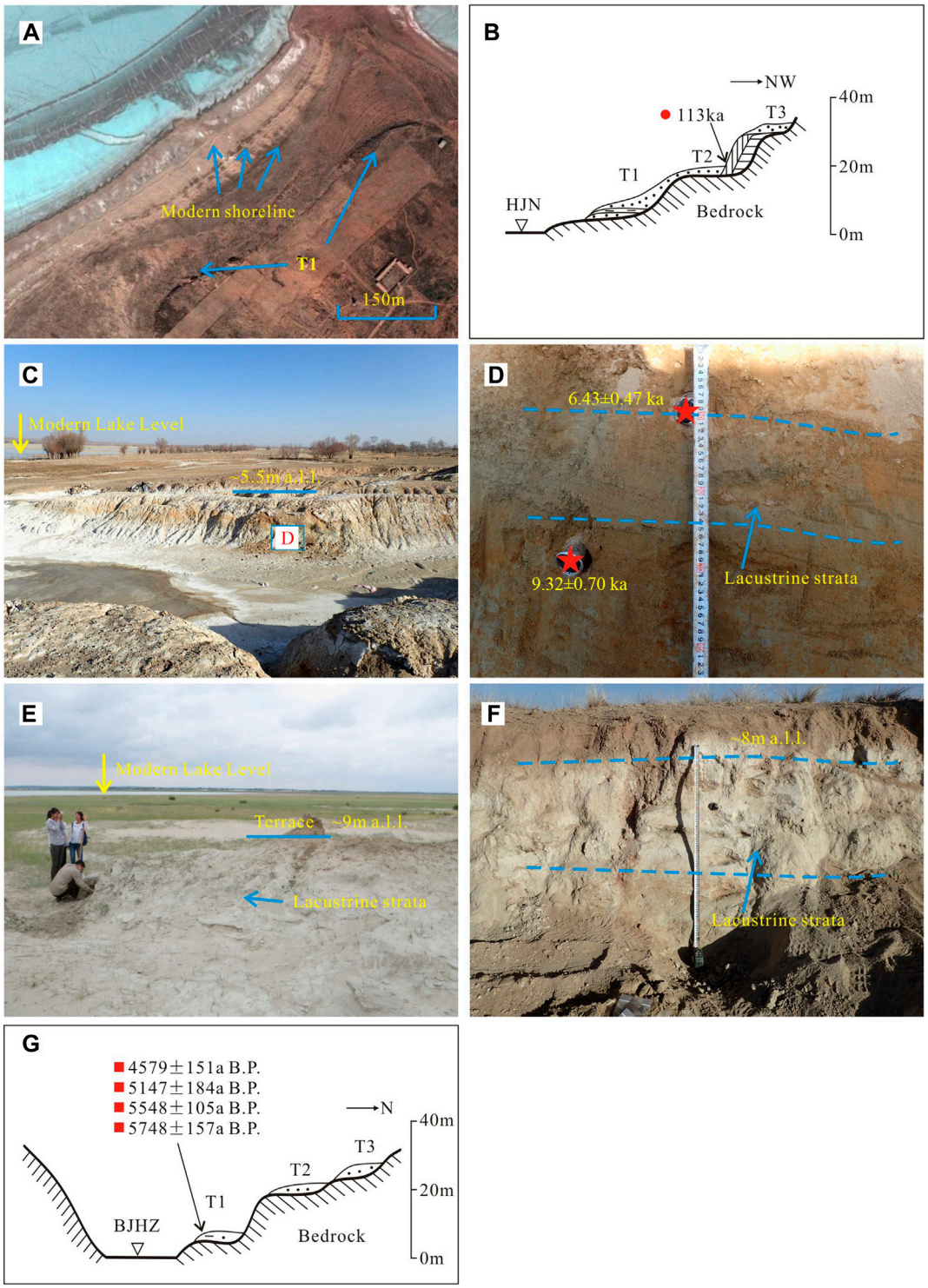

FIGURE 2 | Geomorphology and lacustrine strata of lakes in MUD. **(A)** Image of lake shorelines and T1in south HJN. **(B)** Sketch map of lake terraces of HJN (modified after Shi, 1991). **(C)** Image of lake terrace in the south DLTR. **(D)** Lacustrine strata in the terrace of the south DLTR. **(E)** Holocene lacustrine strata in the southeast beach of BZN. **(F)** Lake terrace and lacustrine strata in the east SRBDY. **(G)** Sketch map of lake terraces in BJHZ (modified after Long et al., 2007; Shi, 1991).The red star, circle, and square show OSL, TL, and ^{14}C dates, respectively. The ^{14}C dates were converted to calendar ages using Calib 7.02 based on the INTCAL 13 calibration (Reimer et al., 2013).

reconstructing high lake levels. The lakes on the Ordos Plateau have been retreating since the late Quaternary. Hongjian Nuur and Bojianghaizi developed three lake terraces (**Figure 2**). T2 and T3 developed before the late Pleistocene, and T1 developed in the early and middle Holocene (Yuan et al., 1987; Shi, 1991). Holocene lake terrace and lacustrine strata in the MUD are generally no more than 10 m higher than the modern lake surface. The lacustrine sediments are gray-white or gray-green silty sand and fine sand with horizontal bedding. The sedimentary texture is loose with poor cementation. The lake terraces are stepped terrain with a flat top and a steep front edge. Lacustrine strata remain partially on the terrace. Based on remote sensing image interpretation, lake basins of Hongjian Nuur (HJN), Dalengturu Nuur (DLTR), Baozhai Nuur (BZN), Sharibuduyin Nuur (SRBDY), and Bojianghaizi (BJHZ) were selected for field investigation and sampling (**Figure 1B**, No.1–5).

HJN is the largest lake in MUD. Shorelines and lake terraces are clearly visible in south HJN. The shorelines formed in recent decades are roughly parallel to the modern shoreline (**Figures 2A,B**). The top of the lacustrine strata in T1 is about 9 m above the modern lake. The sediment is gray-white very fine sand. The terrace of DLTR is in the south of the lake. The terrace is about 5.5 m higher than the modern lake, slightly inclined toward the lake (**Figure 2C**). The lacustrine strata is gray-green fine sand with clay, about 17 cm in thickness (**Figure 2D**). The Holocene terrace of BZN is located on the southeast beach of the lake about 9 m above the modern lake. The lacustrine layer is gray-white silt sand with well-developed horizontal bedding (**Figure 2E**). The lake terrace of SRBDY, located in the east of the lake, is about 8 m higher than the modern lake. The lacustrine strata at the top is about 40 cm, with gray-white fine sand and visible and well-developed horizontal bedding (**Figure 2F**). The T1 in the north of Bojianghaizi is about 7 m higher than the modern lake with gray-green and gray-black lacustrine clay (**Figure 2G**).

Two quartz Optical Stimulated Luminescence (OSL) dating samples were collected in the DLTR section. Pure quartz grains 38–63 μm size were extracted from the middle part of the sample tube using the procedure employed by the OSL Laboratory of the State Key Laboratory of Earth Surface Processes and Resource Ecology, Beijing Normal University. The SAR-SGC method was used to determine the equivalent dose (De) (Lai and Ou, 2013).The measurement equipment was a Risø DA-20 TL/OSL reader equipped with blue diodes (k = 470 ± 20 nm) and a 90Sr/90Y radioactive beta source. The concentrations of Uranium (U), Thorium (Th), and Potassium (K) were measured by inductively coupled plasma mass spectrometry (ICP-MS). The water content was measured by weighing the samples before and after drying. Finally, we obtained the boundary ages of the lacustrine deposit in the DLTR section.

Lake Hydrologic Model

The lake area is governed by lake inputs and outputs. The lake level remains stable when the water inputs equal outputs. Lake inputs are lake surface precipitation and drainage runoffs, whereas the outputs are water surface evaporation and groundwater discharge. Based on the reconstructed lake area, the lake hydrologic model can be used to calculate the precipitation of the corresponding period. The model used in this study followed Goldsmith et al. (2017):

$$P \times A_C \times F_R + P \times A_L = E \times A_L + G \quad (1)$$

where P is mean annual precipitation(m); A_C is the catchment area (m^2) where the area of the lake is subtracted from the area of the catchment; F_R represents the fraction of the watershed precipitation that reaches the lake (including surface and groundwater runoff); A_L is the area of the lake (m^2); E represents the mean annual evaporation of the lake surface (m); and G represents groundwater discharge from the lake per year (m^3).

The catchment area (A_C) was calculated from topographic maps with contour lines of 5 and 10 m. Considering the inter-annual fluctuations of the lake level (Xu et al., 2019), the modern area of the lake (A_L) was averaged from data of two periods: a topographic map drawn in the 1970s and a geomorphic map of the MUD (Wu et al., 2017). The precipitation was interpolated from the mean annual precipitation of meteorological stations in the MUD for 56 years (1961–2016). The highstand area of five lakes was calculated from topographic maps according to the elevation of the lacustrine strata. The watershed area of the lake highstand was the same as the modern catchment area because the elevation of each watershed was much higher than the modern lake and Holocene highstand. All the catchments are closed basins with no hydraulic connection between them. Thus, groundwater discharge from the lake (G) can be neglected for the hydrologic model. The meteorological data of each basin was obtained by interpolation.

The evaporation of the lake surface was estimated using a modified Penman equation (Penman, 1948; Sene et al., 1991):

$$E_d = \frac{\Delta H/L + \gamma E_a}{\Delta + \gamma} \quad (2)$$

where E_d is evaporation per day (m/day); Δ is the slope of the saturation vapor pressure curve at air temperature t (hpa/°C); H is net radiation, J/(m^2·day); L represents latent heat of vaporization (J/kg); γ is psychrometric constant (hpa/°C); and E_a is atmospheric conductance (m/day).

The climatological data (radiation, temperature, air pressure, vapor pressure, wind velocity, and sunshine duration) were obtained from the Chinese Meteorological Agency for the period 1961–2016 for meteorological stations located in the MUD. The mean annual evaporation of each meteorological station was calculated by summing evaporation per day (E_d). The evaporation of each lake surface (E) was mathematically interpolated from these stations. The runoff fraction (F_R) can be calculated using the closed-basin hydrological model. In addition, it can be estimated by the Budyko relationship (Budyko, 1974; Koster et al., 2006):

$$F_R = 1 - E_c/P = 1 - [D(\tanh 1/D)(1 - \cosh D + \sinh D)]^{0.5} \quad (3)$$

where E_c is catchment evaporation calculated as $D = R_{net}/P\ L$, where D is the dryness index, R_{net} is mean annual net radiation, P is annual precipitation, L is latent heat of vaporization, and R_{net}/L is potential evaporation. Potential

TABLE 1 | Quartz OSL ages of lacustrine strata in DLTR.

Sample No.	Lab No.	Depth (m)	Water content (%)	K (%)	U (ppm)	Th (ppm)	De (Gy)	Dose rate (Gy/ka)	Aliquots	Age (ka)
DLTR-2	BNU61	0.69	16.76	3.13 ± 0.05	16.97 ± 0.73	12.41 ± 0.81	41.43 ± 0.64	6.45 ± 0.46	15	6.43 ± 0.47
DLTR-3	BNU62	0.92	12.18	3.00 ± 0.05	11.12 ± 0.51	4.58 ± 0.58	43.76 ± 0.52	4.70 ± 0.35	13	9.32 ± 0.70

evaporation can be measured by the radiative balance or by pan evaporation (Koster et al., 2006; Goldsmith et al., 2017). It also can be approximately estimated using the Penman equation (Yang et al., 2012; Li et al., 2020).In our calculation, the Penman equation was used.

In the modern lake hydrologic model, the mean annual evaporation of meteorological stations in the MUD was calculated using the Penman equation. Then, the evaporation (E) of the five lake basins was calculated by mathematical interpolation. The modern runoff fraction (F_R) of each basin was calculated using the lake hydrologic model and Budyko relationship, respectively. The results show that the two runoff fractions (F_{R1} and F_{R2}) are similar, indicating that both the modern lake hydrological model and Budyko relationship produced suitable estimates.

In this paper, first, the model was applied to HJN, DLTR, BZN, SRBDY, and BJHZ to reconstruct precipitation during the lake highstand. Second, the paleolake areas of other drainages (No. 6–24 in **Figure 1B**) were estimated using this model under the reconstructed precipitation pattern. In the paleolake hydrologic model, the evaporation was also calculated using the Penman equation. Considering the influence of wind speed and temperature on evaporation, we estimated that the evaporation during the lake's highstand was at most 15% higher than the modern value. For the paleolakes, precipitation (or paleolake area) and runoff fraction could not be constrained independently. Therefore, we used both the closed-basin lake hydrologic model and the Budyko relationship to assess these parameters.

Extraction of Published Precipitation Data

A series of precipitation data was extracted from published articles to reconstruct the paleoprecipitation pattern in MUD combining with reconstructed precipitation by the model in **section 3.2**. The published precipitation data were extracted according to the following methods:1) the paleoprecipitation was extracted immediately from articles with exact data; 2) the paleoprecipitation was calculated using modern precipitation (1961–2016) multiplied by change percentage given in the articles; 3) with regard to data in precipitation series, data from the chosen period were digitalized and averaged. With the method above, forty precipitation data was extracted in the MUD and its surrounding region in north China.

RESULTS

Lake Highstand Reconstructed by Lacustrine Landform and Strata

Based on field investigations, the highstand of five lakes was reconstructed using a topographic map and a digital elevation model (**Figure 3**). The area of the paleolakes is 1.65–3.56 times that of modern lakes, with the smallest ratio in HJN. The total area of paleolakes in the five catchments is 158.2 km^2, which is 2.05 times that of modern lakes. There was only one lake during the highstand period in the DLTR and SRBDY drainage. The drainage basins in HJN, BJHZ, and BZN contain more than one lake. In each basin, the elevation of the watershed between lakes is the upper limit of the upstream paleolake level. We also inferred that paleolakes existed in some depressions during the highstand period. For example, the Shejiahaizi (*haizi* means lake in the dialect of study area), located in depression northeast of HJN, was a lake that regressed decades ago according to the topographic map and remote sensing image. During the Holocene highstand period, Shejiahaizi was probably an independent lake that was ~3 m higher than the HJN based on lacustrine landform. In the BZN drainage, lake Baozhai Nuur and the adjacent Baga Nuur were connected to a unified lake due to rising lake levels. In the west of the drainage, there are two depressions where paleolakes may develop. In the BJHZ drainage, two adjacent lakes were connected during the high lake level period.

The quartz optically stimulated luminescence (OSL) ages of the lacustrine strata in DLTR are listed in **Table 1**. The quartz OSL ages confirmed the lake highstand occurred during the early to middle Holocene.

Quantitative Precipitation Reconstruction Based on the Lake Hydrologic Model

The modern precipitation (P), modern and highstand evaporation (E), catchment area (A_C), and runoff fraction (F_R) required in the hydrologic model are listed in **Table 2**. The interpolated modern mean annual evaporation ranged from 995 to 1,065 mm with a rough trend of increasing from east to west. The evaporation of the paleolakes was calculated using modern values multiplied by 1.15. The runoff fraction (F_R) of the paleolake drainages during lake highstand was estimated by Budyko relationship. They ranged from 5% to 8%, higher than at present in each catchment. The runoff fraction (F_R) in both periods shows a decreasing trend from southeast to northwest.

The precipitation of five lakes during the highstand was estimated using the lake hydrologic model (**Table 2**). The reconstructed precipitation of HJN in the eastern MUD was 500 mm. In the middle MUD, the precipitation of BZN and BJHZ was 471 and 472 mm, respectively. The precipitation of DLTR and SRBDY in the west was 443 and 444 mm, respectively. The reconstructed precipitation was 120–165 mm higher than the modern value. The increase in precipitation was 32–60%, and the increase in the west was significantly higher than that in the east.

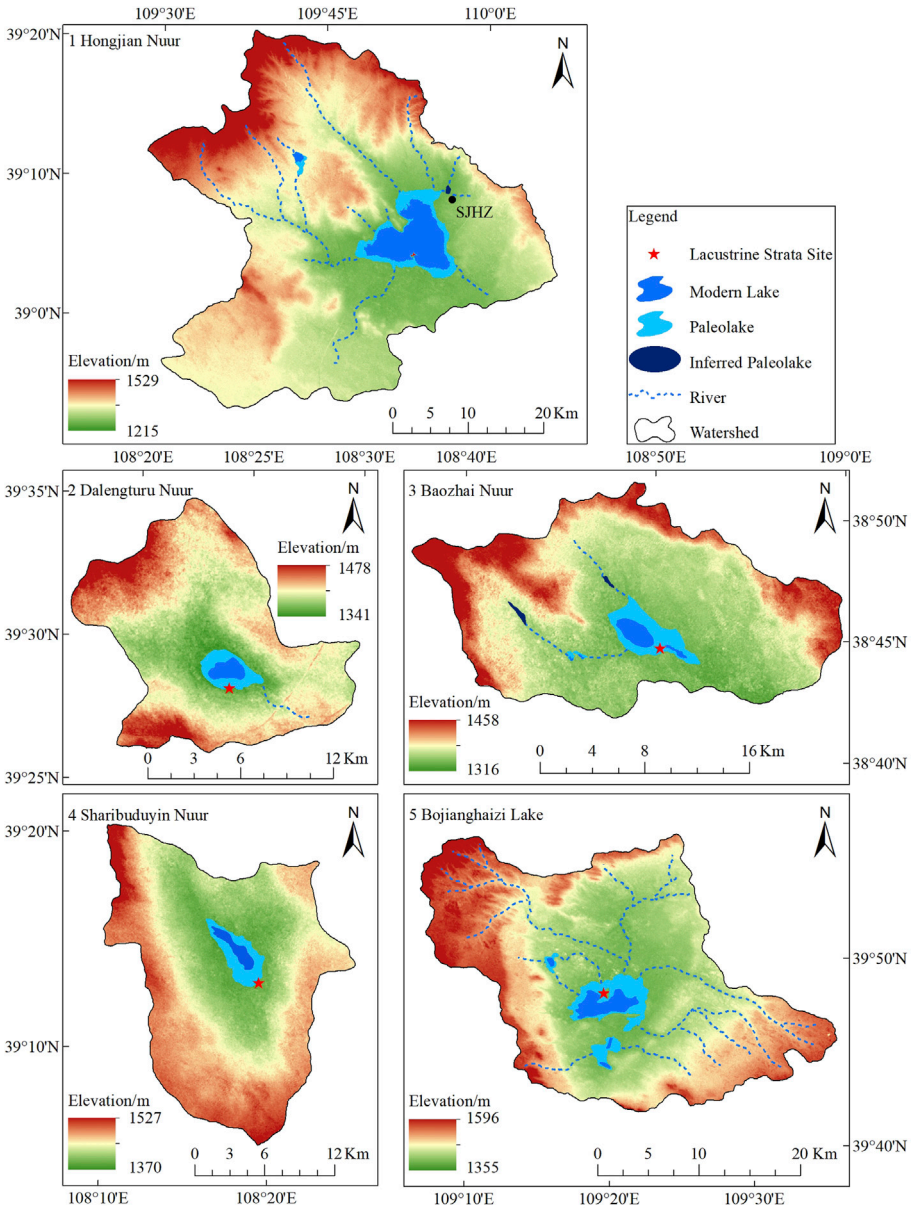

FIGURE 3 | Reconstructed highstand of five lake basins in the MUD (the DEM data is from ASTER GDEM version 2).

Reconstruction of Precipitation Patterns

Precipitation patterns in the MUD during the early to middle Holocene were reconstructed by synthesizing precipitation data in **section 4.2** and published data. A total of forty-five precipitation data from the early to middle Holocene in the MUD and surrounding areas were used (**Supplementary Table S1**). The isohyet of the MUD was reconstructed by interpolation (**Figure 4**). The results show that the precipitation during the early to middle Holocene in the MUD decreased from about 550 mm in the southeast to about 350 mm in the northwest, which is consistent with present levels. The 400 mm isohyet moved 130–170 km to the northwest, roughly consistent with the modern 250 mm isohyet. The moving distance in the southwest is slightly smaller than that in the northeast. The amplification of precipitation gradually increased from southeast to northwest. Due to the difference in amplification, the precipitation gradient in much of the MUD is lower than at present. The large gradient is distributed near the 400 mm isohyet in the west MUD.

Reconstructed Paleolakes

The lake highstand of five drainage areas was reconstructed based on lacustrine landform and strata in **section 4.1**. Based on the reconstructed precipitation pattern in the MUD, the paleolake area of each drainage (No. 6–24) during the early to middle Holocene was estimated. First,

TABLE 2 | The hydrological parameters of each lake basins in the MUD during the modern and highstand period.

No	Name	Period	P/m	E/m	$A_L/10^6m^2$	$A_C/10^6m^2$	F_{R1}/%	F_{R2}/%
1	Hongjian Nuur	Modern	0.380	0.996	54.92	1538.16	6.00	5.94
		Highstand	0.500	1.145	90.36		—	8.04
2	Dalengturu Nuur	Modern	0.288	0.971	2.36	168.36	3.37	3.13
		Highstand	0.443	1.117	6.90		—	6.50
3	Baozhai Nuur	Modern	0.322	1.003	5.29	353.35	3.21	3.87
		Highstand	0.471	1.153	16.15			6.94
4	Sharibuduyin Nuur	Modern	0.279	0.984	3.80	344.28	2.82	2.77
		Highstand	0.444	1.132	13.53		—	6.33
5	Bojianghaizi Lake	Modern	0.317	0.987	10.93	639.00	3.68	3.87
		Highstand	0.472	1.135	31.28		—	7.23
6	Qigai-Baahar Nuur	Modern	0.335	0.995	49.52	2267.19	4.40	4.38
		Highstand	0.485	1.144	119.13		—	7.54
7	Danao Lake	Modern	0.356	0.995	8.67	306.92	5.22	5.09
		Highstand	0.491	1.144	16.88		—	7.74
8	Wulan Nuur	Modern	0.326	0.994	6.16	294.30	4.29	4.09
		Highstand	0.479	1.143	14.82		—	7.35
9	Subei Nuur	Modern	0.314	0.993	15.97	1022.56	3.43	3.72
		Highstand	0.468	1.142	47.38			7.00
10	Hetongchagan Nuur	Modern	0.319	0.998	24.79	1517.12	3.54	3.83
		Highstand	0.476	1.148	73.51		—	7.19
11	Aobai Nuur	Modern	0.319	1.001	15.02	1000.17	3.26	3.80
		Highstand	0.467	1.151	44.61		—	6.84
12	Dakebo Lake	Modern	0.303	0.995	2.88	187.91	3.55	3.37
		Highstand	0.454	1.144	7.71		—	6.50
13	Muduchahan Nuur	Modern	0.301	0.994	7.15	522.60	3.19	3.31
		Highstand	0.453	1.143	21.34		—	6.48
14	Ketuoluohai Nuur	Modern	0.313	0.997	2.51	155.87	3.57	3.65
		Highstand	0.460	1.147	6.67		—	6.67
15	Kaikai Nuur	Modern	0.299	0.992	1.95	155.19	2.94	3.27
		Highstand	0.445	1.141	5.97		—	6.25
16	Haolebaoji Nuur	Modern	0.315	1.003	14.02	978.29	3.18	3.65
		Highstand	0.461	1.153	41.25		—	6.61
17	Baiyan Nuur	Modern	0.294	0.992	3.95	266.11	3.58	3.13
		Highstand	0.445	1.141	10.23		—	6.25
18	Haoqingzhao Nuur	Modern	0.290	0.992	1.15	114.34	2.45	3.01
		Highstand	0.446	1.141	4.43		—	6.29
19	Zhaoshao Lake	Modern	0.276	0.993	1.57	166.12	2.49	2.62
		Highstand	0.405	1.142	4.43		—	4.98
20	Nalin Nuur	Modern	0.285	0.985	3.11	236.37	3.27	2.93
		Highstand	0.416	1.133	7.21		—	5.42
21	Hadatu Nuur	Modern	0.290	0.988	2.33	177.96	3.19	3.05
		Highstand	0.434	1.136	6.32		—	5.95
22	Wuhudong Nuur	Modern	0.264	1.025	15.38	2638.69	1.69	2.11
		Highstand	0.418	1.179	70.29		—	4.98
23	Beidachi Lake	Modern	0.281	1.034	12.13	1397.54	2.35	2.46
		Highstand	0.475	1.189	58.81		—	6.60
24	Gouchi Lake	Modern	0.307	1.065	35.52	3751.55	2.36	2.90
		Highstand	0.509	1.236	176.88		—	7.07

F_{R1} and F_{R2} represent runoff fractions calculated by the lake hydrologic model and Budyko relationship, respectively.

the runoff fraction (F_{R2}) of each drainage basin was estimated using the Budyko relationship. Second, the lake area of each basin was calculated using the lake hydrologic model (**Table 2**). The total area of reconstructed paleolakes during the early to middle Holocene was 896.1 km^2, which is 2.96 times that of modern lakes. The lake area of each drainage is two to five times that of modern lakes with the largest increase in the southwest MUD. The area of the paleolake in the Wuhudong Nuur, Gouchi, and Beidachi basins (No. 22–24 in **Table 2**) are 4.57, 4.84, and 4.97 times that of modern lakes, respectively.

Based on the reconstructed lake area in each drainage (No. 6–24), we also attempted to reconstruct the paleolake pattern. For the catchment comprising one single lake, the paleolake expanded by topographic contour around the modern lake based on the calculated area. In the basin comprising a series of catenulated lakes, the elevation of the watershed between lakes was regarded as the altitude of the paleolake upstream. The upstream paleolake area was calculated using closed contour and the corresponding altitude. The downstream lake area was calculated as the total area minus the upstream lake area. Due to the rise in lake levels, adjacent lakes may have become unified lakes. Therefore, the

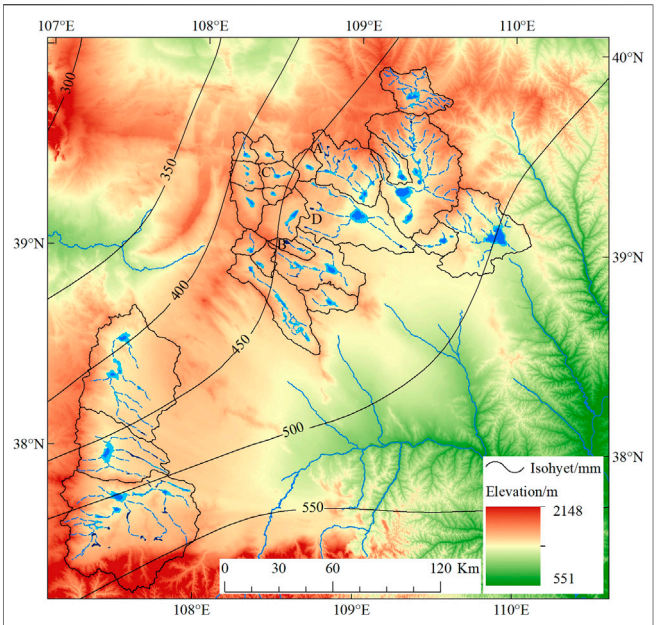

FIGURE 4 | Reconstructed precipitation and lake pattern in the MUD (the legends are same as **Figure 3**).

modern 108 lakes decreased to eighty-four during the early to middle Holocene. In addition, there are small, closed depressions in certain catchments. These depressions were inferred as paleolakes during the Holocene highstand. A total of forty-three inferred lakes with an area more than 0.1 km^2 were identified. According to the method above, there were 127 paleolakes in the closed flow area of MUD during the early to middle Holocene. The paleolake pattern is shown in **Figure 4**.

DISCUSSION

Estimation of Evaporation Used in the Lake Hydrologic Model

As one of the required parameters in the lake hydrologic model, open water evaporation is typically estimated by observing different pans. However, the observation data of a 20 m^2 evaporation pan, which is approximately equal to open water evaporation, is rare in the MUD. The observation data of D20 and 601B pans are significantly higher than open water evaporation in arid and semi-arid areas because of the pan wall. In certain regions, open water evaporation is estimated using observation data of pans multiplied by a conversion coefficient (Linacre, 1994). However, the conversion coefficient in the MUD was difficult to constrain. Therefore, a modified Penman equation was used to estimate the evaporation of the lake surface (Penman, 1948; Sene et al., 1991). The Penman equation has been used to calculate evaporation in arid and semi-arid China (Li et al., 2001; Yang et al., 2010). The difference between calculated values and measured data in 20 m^2 evaporation pans was no more than 10% according to experiments conducted in the arid regions of Xinjiang, in western China (Zhang and Zhou, 1992).

TABLE 3 | Evaporation of meteorological station in MUD.

Station	Mean annul			Mean May to September[b]		
	E_{D20}/mm[a]	E/mm	E_{D20}/ E	E_{601B}/mm	E/mm	E_{601B}/ E
Shenmu	1914.4	1000.6	0.52	690.8	673.1	0.97
Jingbian	1967.5	992.7	0.50	759.9	703.3	0.93
Yanchi	2042.0	1009.1	0.49	782.6	695.6	0.89
Hengshan	2084.4	1009.6	0.48	803.4	684.7	0.85
Suide	2108.2	1013.8	0.48	794.4	702.2	0.88
Dingbian	2289.0	1089.3	0.48	888.1	734.1	0.83
Dongsheng	2259.5	971.2	0.43	789.3	693.0	0.88
Otog	2453.2	979.2	0.40	835.9	681.1	0.81

[a]*E_{D20} and E_{601B} represent observation data of D20 and 601B pans, respectively.*
[b]*The 601B pan is generally used during May to September since 2002 in the MUD.*

The observed evaporation of two pans and calculated evaporation using the Penman equation are listed in **Table 3**. The ratios E_{D20}/E and E_{601B}/E are 0.4–0.52 and 0.81–0.97, respectively. Both ratios decreased from the semi-arid southeast to the arid northeast. The average conversion coefficient between D20 pan and open water evaporation in arid northwest China and Inner Mongolia Plateau was estimated at 0.44 and 0.52, respectively (Xie and Wang, 2007). The E_{D20}/E ratio in the MUD was roughly between these two coefficients. The conversion coefficient between 601B pan and 20 m^2 pan in North China ranged from 0.83 to 0.93, which is close to the E_{601B}/E ratio in the MUD. The decreasing trend from semi-humid Henan to semi-arid Inner Mongolia was also consistent with the MUD (Qian et al., 1998). This indicates the evaporation calculated using the Penman equation was approximately equal to the open water evaporation.

In the paleolake hydrologic model, the evaporation of lakes was also estimated using the Penman equation. The temperature during the early to middle Holocene was about 1°C higher than modern times (Fang et al., 2011). Based on the sensitivity of evaporation to temperature change, a 1°C rise would produce evaporation rate changes of about 5–6% in the MUD. We also examined the sensitivity of evaporation to wind speed change. A 20% change in wind speed can lead to about a 10% change in evaporation, which is nearly consistent with the examination in Dali Lake in eastern Inner Mongolia (Goldsmith et al., 2017). Thus, considering the possible change in temperature and wind speed, the evaporation was assumed at 15% higher than the modern value at most.

Reconstructed Precipitation in the MUD

The lake hydrologic model is one of the common methods for reconstructing precipitation. The precipitation reconstructed in HJN was 500 mm. The result is approximate to the value 510 ± 25 mm estimated from pollen data from the Hejialiang section about 15 km east of the lake (Chen et al., 1993). The reconstructed precipitation in BZN was 471 mm. The rainfall calculated based on pollen assemblage in Taobao and Wushen profiles was 470 ± 25 and 461.8 mm, respectively (Shi, 1991; Chen et al., 1993). These two profiles are about 7 and 15 km to the southeast of BZN, respectively. This indicated that the lake hydrologic model and pollen assemblage produced suitable estimates. The mean annual

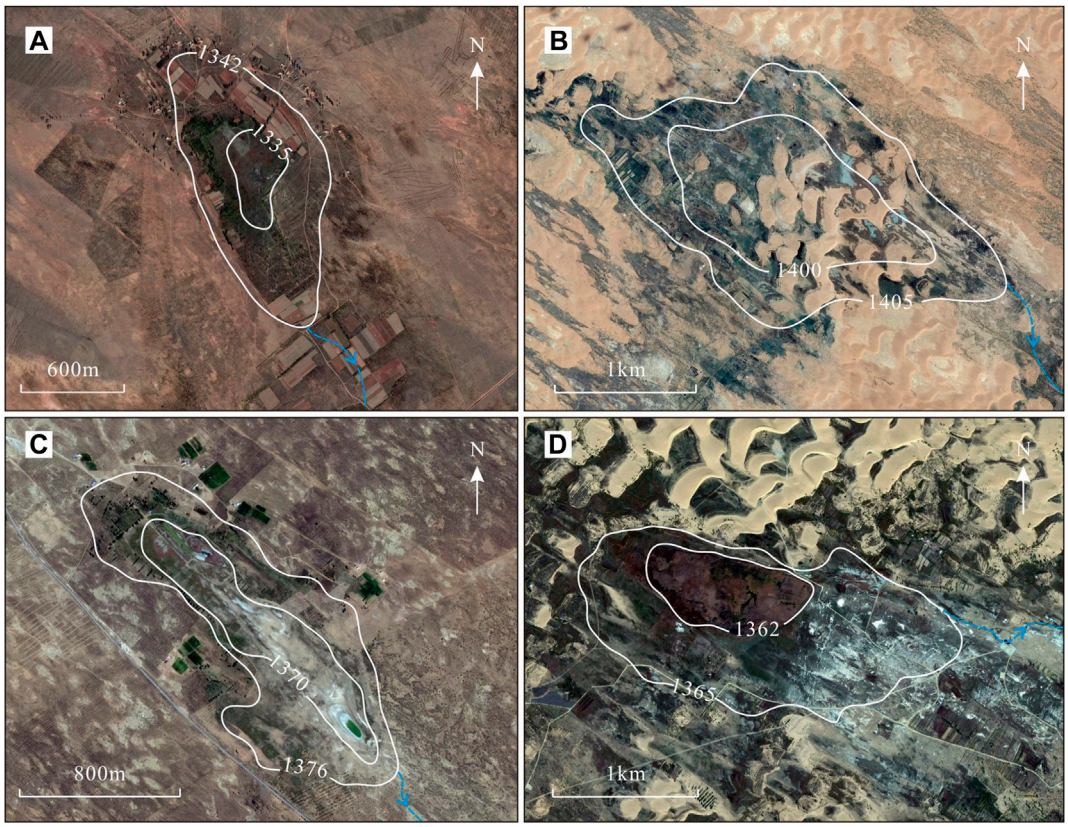

FIGURE 5 | Inferred paleolake in the MUD during the early to middle Holocene (The white curves represent contour lines extracted from topographic maps, the number means elevation/m. The blue line with arrow indicates the possible flow direction. **(A–D)** correspond to locations in **Figure 4**).

precipitation of the HJN lake was ~380 mm. The precipitation during the early to middle Holocene was ~32% higher than present. The result is consistent with reconstructed results near the 400 mm isohyet in the MUD and southeast Inner Mongolia Plateau (Jiang et al., 2006; Xu et al., 2010). However, the result was much smaller than the estimated precipitation of Qinghai Lake (Shi et al., 1992). This may reflect that the migration distance of the monsoon rain belt varied in different regions of the monsoon edge area.

In the EASM area of China, the relative increase in precipitation during the early to middle Holocene varied from ~10 to 15% in the humid southeastern coastal area to more than 70% in the arid northwest area (Yang and Williams, 2003; Stebich et al., 2015; Liu and Li, 2017; Li et al., 2018; Wu et al., 2018). The reconstructed relative increase in the MUD rose from ~32% in the southeast to ~60% in the northwest. The rising trend is consistent with the whole EASM area in China. However, the extent of relative increase ranges significantly from southeast to the northwest, indicating that the monsoon edge area was extremely sensitive to climatic change. During the early to middle Holocene, the precipitation gradient decreased significantly in the MUD due to the difference in precipitation increase. This probably reflects the monsoon rain belt and the monsoon edge area migration to the northwest. In consequence, the MUD was stably dominated by the EASM. The spatio-temporal pattern of climate showed a relatively stable, warm, and humid climate for millennia. It can also be confirmed from the peat and paleosol development process in the MUD. The development of peat and lacustrine in the MUD since the last deglaciation indicates the regional climate fluctuated considerably until 8.5 ka. Thereafter there were humid intervals until 6ka, during which lacustrine sediments were deposited (Liu et al., 2018b). The paleosol was generally regarded as the indicator of warm and humid climate. In the aeolian sand/paleosol sequence of the MUD, the duration of paleosol is much longer than the aeolian sand during the early to middle Holocene (Gao et al., 1993; Ding et al., 2021).

Paleolake Pattern in the Closed Drainage Area

The lakes in northern China generally reached their highstand due to the increase in precipitation in the early and middle Holocene. The lake landforms and lacustrine strata of HJN and BJHZ are direct evidence of the development of high lakes in the study area. The decrease in the grain size of lacustrine deposits in the lake cores of the Baahar Nuur and Qigai Nuur in north MUD indicates an increase in lake level during the early and middle Holocene (Guo et al., 2007; Sun and

Feng, 2013). The clay deposits in Chagan Nuur in the western MUD indicate a stable deep-water sedimentary environment of ~9–5 ka (Yang, 1997). Clay sediments in Hetongchahagan Nuur in the western MUD indicate a stable deep-water sedimentary environment at~9—6 ka (Bernasconi et al., 1997). Grain size analysis of the DSGL profile in the southern MUD showed that the Salawusu Lake began to form in the early Holocene and reached its maximum in the middle Holocene (Liu et al., 2018b). These lake records above indicate that the lake highstands during the early to middle Holocene in the MUD were almost simultaneous and stable.

The total area of lakes in the closed drainage area is 2.96 times that of modern lakes. The relative height between the highstand and the modern lake surface is about 5–9 m. The increase of height and area was smaller than the lakes in Badain Jaran Desert and Tengger Desert (Yang and Williams, 2003; Zhang et al., 2004). Most of the lakes in the study area locate in bedrock valleys or aeolian bedrock depressions. The topography of the lake basins is mainly controlled by bedrock gullies. The modern aeolian activity has little impact on topography. The stable terrain is conducive to the reconstruction of paleolake pattern. According to the reconstruction results, the number of paleolakes increased along with the rise of the lake level and the expansion of the lake area. The adjacent lakes in certain basins connected and formed unified lakes due to the rise in water level. In addition, closed depressions were extracted from topographic maps and remote sensing images. Geomorphic relics, such as lake shorelines, can be distinguished around the depressions. Salt crystals on the surface of depressions indicated paleolakes may have existed (**Figure 5**). We inferred these closed depressions formed lakes due to the rise of precipitation during the early to middle Holocene. In each catchment, the altitude of the lake highstands was lower than the watershed between drainages. The pattern of closed drainage area is consistent with the present. There is no evidence from the lake landform, lacustrine strata, and climatic conditions supporting the formation of a unified megalake in the closed drainage area during the early to middle Holocene.

CONCLUSION

The precipitation and lake areas of the MUD during the early and middle Holocene were quantitatively reconstructed based on the lacustrine landform, and by using the lake hydrologic model. A total of 127 paleolakes existed in the closed flow area during the early to middle Holocene. The paleolake area was 896.1 km^2, which is 2.96 times that of modern lakes. The relative height between the highstand and the modern lake surface is about 5–9 m. The precipitation during early to middle Holocene decreased from about 550 mm in the southeast to about 350 mm in the northwest. The 400 mm isohyet moved 130–170 km to the northwest, roughly consistent with the modern 250 mm isohyet. The relative increase in precipitation was ~32–60%, and the increase in the west was significantly higher than the east. The precipitation gradient in much of the MUD was lower than the present. The results above indicate that the monsoon edge area and monsoon rain belt have migrated to the northwest. Furthermore, the MUD was stably dominated by the EASM. The spatio-temporal pattern of the climate during the early to middle Holocene was relatively warm and humid with a decreased precipitation gradient for millennia.

DATA AVAILABILITY STATEMENT

The original contributions presented in the study are included in the article/**Supplementary Material**, further inquiries can be directed to the corresponding author.

AUTHOR CONTRIBUTIONS

DL, YWu, and LT contributed to conception and design of the study. DL, LT, YWe, and TF conducted investigation and methodology. DL, YWe, and TF performed the statistical analysis. YWu provided the funding. All authors contributed to manuscript revision, read, and approved the submitted version.

SUPPLEMENTARY MATERIAL

The Supplementary Material for this article can be found online at: https://www.frontiersin.org/articles/10.3389/feart.2022.850633/full#supplementary-material

REFERENCES

An, Z., Porter, S. C., Kutzbach, J. E., Wu, X. H., Wang, S. M., Liu, X. D., et al. (2000). Asynchronous Holocene Optimum of the East Asian Monsoon. *Quat. Sci. Rev.* 19, 743–762. doi:10.1016/S0277-3791(99)00031-1

Bernasconi, S. M., Dobson, J., Mckenzie, J. A., Ariztegui, D., Niessen, F., Hsu, K. J., et al. (1997). Preliminary Isotopic and Palaeomagnetic Evidence for Younger Dryas and Holocene Climate Evolution in NE Asia. *Terra Nova* 9 (5-6), 246–250. doi:10.1046/j.1365-3121.1997.d01-38.x

Budyko, M. I. (1974). *Climate and Life*. San Diego: Academic Press.

Chen, F., Li, G., Zhao, H., Jin, M., Chen, X., Fan, Y., et al. (2014). Landscape Evolution of the Ulan Buh Desert in Northern China during the Late Quaternary. *Quat. Res.* 81, 476–487. doi:10.1016/j.yqres.2013.08.005

Chen, F., Xu, Q., Chen, J., Birks, H. J. B., Liu, J., Zhang, S., et al. (2015). East Asian Summer Monsoon Precipitation Variability since the Last Deglaciation. *Sci. Rep.* 5, 1–11. doi:10.1038/srep11186

Chen, W. N., Gao, S. Y., Shao, Y. J., and Zhang, H. L. (1993). Palynological Assemblages and Paleoclimatic Change of Mu Us Sandy Land during Holocene. *J. Chin. Hist. Geogr.* 14 (01), 22–30.

Cohen, A. S. (2003). *Paleolimnology: The History and Evolution of Lake Systems*. Oxford, England: Oxford University Press.

Department of Geography of Peking University (1983). *Natural Features and Rehabilitation of Mu Us Sandy Land*. Beijing: Science Press.

Ding, Z., Lu, R., Wang, L., Yu, L., Liu, X., Liu, Y., et al. (2021). Early-mid Holocene Climatic Changes Inferred from Colors of Eolian Deposits in the Mu Us Desert. *Geoderma* 401, 115172. doi:10.1016/j.geoderma.2021.115172

Fang, X. Q., Liu, C. H., and Hou, G. L. (2011). Reconstruction of Precipitation Pattern of China in the Holocene Megathermal. *Scientia Geographica Sinica* 31 (11), 1287–1292. doi:10.13249/j.cnki.sgs.2011.011.1287

Fritz, S. C. (2008). Deciphering Climatic History from Lake Sediments. *J. Paleolimnol* 39, 5–16. doi:10.1007/s10933-007-9134-x

Gao, S. Y., Chen, W. N., Jin, H. L., Dong, G. R., Li, B. S., Yang, G. S., et al. (1993). A Preliminary Study on Desert Evolution in the Northwestern Fringe of Monsoon Area. *China. Sci. China, Ser. B.* 23 (2), 202–208. doi:10.3321/j.issn:1006-9240.1993.02.005

Goldsmith, Y., Broecker, W. S., Xu, H., Polissar, P. J., DeMenocal, P. B., Porat, N., et al. (2017). Northward Extent of East Asian Monsoon Covaries with Intensity on Orbital and Millennial Timescales. *Proc. Natl. Acad. Sci. USA* 114, 1817–1821. doi:10.1073/pnas.1616708114

Guo, L., Feng, Z., Li, X., Liu, L., and Wang, L. (2007). Holocene Climatic and Environmental Changes Recorded in Baahar Nuur Lake Core in the Ordos Plateau, Inner Mongolia of China. *Chin. Sci Bull* 52, 959–966. doi:10.1007/s11434-007-0132-1

Hou, G. C., Zhang, M. S., Liu, F., Wang, Y. H., Liang, Y. P., Tao, Z. P., et al. (2005). *Groundwater Exploration and Research in the Ordos Basin*. Beijing: Geological Publishing House.

Hou, G. C., Zhao, Z. H., Wang, X. Y., Gong, B., and Yin, L. H. (2008). Formation Mechanism of Interior Drainage Areas and Closed Drainage Areas of the Ordos Plateau in the Middle Reaches of the Yellow River, China Based on an Analysis of the Water Cycle. *Geol. Bull. China* 27 (8), 1107–1114. doi:10.3969/j.issn.1671-2552.2008.08.002

Jia, F., Lu, R., Gao, S., Li, J., and Liu, X. (2015). Holocene Aeolian Activities in the Southeastern Mu Us Desert, China. *Aeolian Res.* 19, 267–274. doi:10.1016/j.aeolia.2015.01.002

Jia, F., Lu, R., Liu, X., Zhao, C., Lv, Z., and Gao, S. (2018). Palaeoenvironmental Implications of a Holocene Sequence of Lacustrine-Peat Sediments from the Desert-Loess Transitional Zone in Northern China. *J. Asian Earth Sci.* 156, 167–173. doi:10.1016/j.jseaes.2018.01.030

Jiang, W., Guo, Z., Sun, X., Wu, H., Chu, G., Yuan, B., et al. (2006). Reconstruction of Climate and Vegetation Changes of Lake Bayanchagan (Inner Mongolia): Holocene Variability of the East Asian Monsoon. *Quat. Res.* 65 (3), 411–420. doi:10.1016/j.yqres.2005.10.007

Koster, R. D., Fekete, B. M., Huffman, G. J., and Stackhouse, P. W. (2006). Revisiting a Hydrological Analysis Framework with International Satellite Land Surface Climatology Project Initiative 2 Rainfall, Net Radiation, and Runoff Fields. *J. Geophys. Res.* 111. doi:10.1029/2006JD007182

Lai, Z. P., and Ou, X. J. (2013). Basic Procedures of Optically Stimulated Luminescence (OSL) Dating. *Prog. Geogr.* 32 (5), 683–693. doi:10.11820/dlkxjz.2013.05.001

Li, G., Wang, Z., Zhao, W., Jin, M., Wang, X., Tao, S., et al. (2020). Quantitative Precipitation Reconstructions from Chagan Nur Revealed Lag Response of East Asian Summer Monsoon Precipitation to Summer Insolation during the Holocene in Arid Northern China. *Quat. Sci. Rev.* 239, 106365. doi:10.1016/j.quascirev.2020.106365

Li, J., Dodson, J., Yan, H., Wang, W., Innes, J. B., Zong, Y., et al. (2018). Quantitative Holocene Climatic Reconstructions for the Lower Yangtze Region of China. *Clim. Dyn.* 50, 1101–1113. doi:10.1007/s00382-017-3664-3

Li, W. C., Li, S. J., and Pu, P. M. (2001). Estimates of Plateau Lake Evaporation:A Case Study of Zige Tangco. *J. Lake Sci.* 13, 227–232. doi:10.18307/20010305

Linacre, E. T. (1994). Estimating U.S. Class A Pan Evaporation from Few Climate Data. *Water Int.* 19, 5–14. doi:10.1080/02508069408686189

Liu, X., Lu, R., Lü, Z., Du, J., Jia, F., Li, T., et al. (2017). Magnetic Susceptibility of Surface Soils in the Mu Us Desert and its Environmental Significance. *Aeolian Res.* 25, 127–134. doi:10.1016/j.aeolia.2017.04.003

Liu, X., Lu, R., Jia, F., Chen, L., Li, T., Ma, Y., et al. (2018a). Holocene Water-Level Changes Inferred from a Section of Fluvio-Lacustrine Sediments in the Southeastern Mu Us Desert, China. *Quat. Int.* 469, 58–67. doi:10.1016/j.quaint.2016.12.032

Liu, X., Lu, R., Du, J., Lyu, Z., Wang, L., Gao, S., et al. (2018b). Evolution of Peatlands in the Mu Us Desert, Northern China, since the Last Deglaciation. *J. Geophys. Res. Earth Surf.Earth Surf.* 123, 252–261. doi:10.1002/2017JF004413

Liu, Y., and Li, Y. (2017). Quantitative Reconstruction of Precipitation and Runoff during MIS 5a, MIS 3a, and Holocene, Arid China. *Theor. Appl. Climatol* 130, 747–754. doi:10.1007/s00704-016-1921-8

Long, H., Wang, N. A., Li, Y., and Wang, C. H. (2007). Particle Size Characteristics of Deposits from PJHZ Section in Northern Edge of Mu Us Desert and Their Environmental Significance. *J. Desert Res.* 27 (02), 187–193. doi:10.3321/j.issn:1000-694X.2007.02.004

Penman, H. L. (1948). Natural Evaporation from Open Water, Bare Soil and Grass. *Proc. R. Soc. Lond. A.* 193, 120–145. doi:10.1098/rspa.1948.0037

Qian, Y. P., Wang, L., Li, W. Y., and Lin, Y. P. (1998). Water-surface Evaporation Research in Bayangaole Evaporation Experimental Station, Inner Mongolia. *J. China Hydrol.* 04, 35–38.

Reimer, P. J., Bard, E., Bayliss, A., Beck, J. W., Blackwell, P. G., Ramsey, C. B., et al. (2013). IntCal13 and Marine13 Radiocarbon Age Calibration Curves 0-50,000 Years Cal BP. *Radiocarbon* 55, 1869–1887. doi:10.2458/azu_js_rc.55.16947

Sene, K. J., Gash, J. H. C., and McNeil, D. D. (1991). Evaporation from a Tropical Lake: Comparison of Theory with Direct Measurements. *J. Hydrol.* 127, 193–217. doi:10.1016/0022-1694(91)90115-x

Shi, P. J., Jiang, T. M., and Liu, Q. F. (1988). Reconstruction of Precipitation during the Last Stage of the Late Pleistocene and the Middle Holocene in Ordos Plateau of North China. *J. Beijing Normal Univ. (Natural Science)* 24, 94–99.

Shi, P. J. (1991). *Theory and Practice of Research into Geography Environment Changes—Research into Geographical Environment Change during Late Quaternary Period in the Ordos Region of North China*. Beijing: Science Press.

Shi, Y. F., Kong, Z. C., Wang, S. M., Tang, L. Y., Wang, F. B., Yao, T. D., et al. (1992). The Climatic Fluctuation and Important Events of Holocene Megathermal in China. *Sci. China Ser. B* 22 (12), 1300–1308. doi:10.1360/zb1992-22-12-1300

Stebich, M., Rehfeld, K., Schlütz, F., Tarasov, P. E., Liu, J., and Mingram, J. (2015). Holocene Vegetation and Climate Dynamics of NE China Based on the Pollen Record from Sihailongwan Maar Lake. *Quat. Sci. Rev.* 124, 275–289. doi:10.1016/j.quascirev.2015.07.021

Sun, A., and Feng, Z. (2013). Holocene Climatic Reconstructions from the Fossil Pollen Record at Qigai Nuur in the Southern Mongolian Plateau. *The Holocene* 23, 1391–1402. doi:10.1177/0959683613489581

Sun, D. H., Zhou, J., Wu, X. H., and Porter, S. C. (1995). Preliminary Reconstruction of Annual Rainfall in Loess Plateau and Loess-Desert Transitional Regions in Suitable Climatic Period of Holocene. *J. Desert Res.* 15 (4), 339–344. doi:10.3321/j.issn:1000-694X.1995.04.012

Wan, Y. Y., Su, X. S., Dong, W. H., and Hou, G. C. (2010). Evaluation of Groundwater Renewal Ability in the Ordos Cretaceous Groundwater Basin. *J. Jilin Univ. (Earth Sci. Edition)* 40 (03), 623–630. doi:10.3969/j.issn.1671-5888.2010.03.020

Wang, N., Ning, K., Li, Z., Wang, Y., Jia, P., and Ma, L. (2016). Holocene High Lake-levels and Pan-lake Period on Badain Jaran Desert. *Sci. China Earth Sci.* 59, 1633–1641. doi:10.1007/s11430-016-5307-7

Wang, S. M., and Dou, H. S. (1998). *Lakes in China*. Beijing: Science Press.

Wu, Y. Q., Tan, L. H., Hao, C. Z., Fu, T. Y., Zhang, M., Wen, Y. L., et al. (2017). *Geomorphic Map of Mu Us Desert*. Harbin: Harbin Cartographic Publishing House.

Wu, Y. L., Wang, Y. B., Liu, X. Q., Yu, Z. T., and Ni, Z. Y. (2018). Holocene Climate Evolution in the Monsoonal Margin Region Revealed by the Pollen Record from Jilantai Playa. *J. Lake Sci.* 30 (4), 1161–1176. doi:10.18307/2018.0427

Xie, X. Q., and Wang, L. (2007). Changes of Potential Evaporation in Northern China over the Past 50 Years. *J. Nat. Resour.* 22 (05), 683–691. doi:10.11849/zrzyxb.2007.05.002

Xu, D. L., Ding, J. N., and Wu, Y. Q. (2019). Lake Area Change in the Mu Us Desert in 1989-2014. *J. Desert Res.* 39 (06), 40–47. doi:10.7522/j.issn.1000-694X.2018.00099

Xu, Q., Xiao, J., Li, Y., Tian, F., and Nakagawa, T. (2010). Pollen-based Quantitative Reconstruction of Holocene Climate Changes in the Daihai Lake Area, Inner Mongolia, China. *J. Clim.* 23, 2856–2868. doi:10.1175/2009JCLI3155.1

Yang, Q. T. (1997). Basic Sedimentary Characters and Paleoclimatic Implications of Saline Lakes in Inner Mongolia. *Geology. Chem. Minerals* 19 (01), 50–54.

Yang, S., Ding, Z., Li, Y., Wang, X., Jiang, W., and Huang, X. (2015a). Warming-induced Northwestward Migration of the East Asian Monsoon Rain Belt from the Last Glacial Maximum to the Mid-holocene. *Proc. Natl. Acad. Sci. USA* 112, 13178–13183. doi:10.1073/pnas.1504688112

Yang, X., Ma, N., Dong, J., Zhu, B., Xu, B., Ma, Z., et al. (2010). Recharge to the Inter-dune Lakes and Holocene Climatic Changes in the Badain Jaran Desert, Western China. *Quat. Res.* 73, 10–19. doi:10.1016/j.yqres.2009.10.009

Yang, X., Scuderi, L. A., Wang, X., Scuderi, L. J., Zhang, D., Li, H., et al. (2015b). Groundwater Sapping as the Cause of Irreversible Desertification of Hunshandake Sandy Lands, Inner Mongolia, Northern China. *Proc. Natl. Acad. Sci. USA* 112 (3), 702–706. doi:10.1073/pnas.1418090112

Yang, X., Scuderi, L., Paillou, P., Liu, Z., Li, H., and Ren, X. (2011). Quaternary Environmental Changes in the Drylands of China - A Critical Review. *Quat. Sci. Rev.* 30, 3219–3233. doi:10.1016/j.quascirev.2011.08.009

Yang, X., and Williams, M. A. J. (2003). The Ion Chemistry of Lakes and Late Holocene Desiccation in the Badain Jaran Desert, Inner Mongolia, China. *Catena* 51, 45–60. doi:10.1016/s0341-8162(02)00088-7

Yang, Z. C., Li, Y. L., Cui, D., Chen, J., and Zhao, X. Y. (2012). Changes of Main Climatic Parameters and Potential Evapotranspiration in Typical Semi-arid Sandy Lands of Northern China during 1951-2005. *J. Desert Res.* 32 (5), 1384–1392.

Yuan, B. Y., Cui, J. X., and Yin, Q. (1987). The Relationship between Gully Development and Climatic Changes in the Loess Yuan Region: Examples from Luochuan, Shaanxi Province. *Acta Geographica Sinica* 42 (4), 328–337. doi:10.11821/xb198704005

Zhang, G. W., and Zhou, Y. C. (1992). Evaporation Properties and Estimates in the Landlocked Arid Region in Xinjiang. China. *Adv. Water Sci.* 3, 226–232. doi:10.3321/j.issn:1001-6791.1992.03.010

Zhang, H. C., Peng, J. L., Ma, Y. Z., Chen, G. J., Feng, Z.-D., Li, B., et al. (2004). Late Quaternary Palaeolake Levels in Tengger Desert, NW China. *Palaeogeogr. Palaeoclimatol. Palaeoecol.* 211, 45–58. doi:10.1016/j.palaeo.2004.04.006

Zhang, J., Tsukamoto, S., Jia, Y., and Frechen, M. (2016). Lake Level Reconstruction of Huangqihai Lake in Northern China since Mis 3 Based on Pulsed Optically Stimulated Luminescence Dating. *J. Quat. Sci.* 31, 225–238. doi:10.1002/jqs.2861

Zhang, L. S., Shi, P. J., Hou, L. F., and Fang, X. Q. (1993). "Research on Precipitation Change and its Distributive Pattern of Monsoon Edge Area in Northern China during Holocene Period," in *Research on the Past Life-Supporting Environment Change of China(I)*. Editor L S Zhang (Beijing: Ocean Press), 147–154.

Zheng, X. Y., Zhang, M. G., Dong, J. H., Gao, Z. H., Xu, C., Han, Z. M., et al. (1992). *Salt Lakes in Inner Mongolia*. Beijing: Science Press.

Zhou, W., Head, M. J., Lu, X., An, Z., Jull, A. J. T., and Donahue, D. (1999). Teleconnection of Climatic Events between East Asia and Polar, High Latitude Areas during the Last Deglaciation. *Palaeogeogr. Palaeoclimatol. Palaeoecol.* 152, 163–172. doi:10.1016/S0031-0182(99)00041-3

Zhu, Z. D., Wu, Z., Liu, S., and Di, X. (1980). *An Outline of Chinese Deserts*. Beijing: Science Press.

Conflict of Interest: The authors declare that the research was conducted in the absence of any commercial or financial relationships that could be construed as a potential conflict of interest.